iScience, Volume *26*

Supplemental information

Adeno-associated virus vector system controlling capsid expression improves viral quantity and quality

Kenji Ohba, Yoshihide Sehara, Tatsuji Enoki, Junichi Mineno, Keiya Ozawa, and Hiroaki Mizukami

Supplemental information

Supplementary Figure 1. Transfection efficiency between normal and Tet-Cap systems during AAV vector production

Difference in transfection efficiency in the normal control (RC2) and Tet-Cap2 systems. Transfection was performed as indicated in Figure 2C and the STAR Methods section. Cells were observed at 24 h post-transfection using fluorescence microscopy. The green color (EGFP expression) indicates transfected cells, and bright field show all cells in the plates. White bar shows 100 μm. Data indicate representative images from three independent experiments.

Supplementary Figure 2. Effect of AAV vector production in the Tet-Cap system for various serotypes

(A-D) AAV vector yield of various serotypes for the Tet-Cap system. Fold difference of AAV vector yield for AAV1 (A), AAV3B (B), AAV5 (C), and AAV6 (D) after a change in medium and doxycycline stimulation at 12h post-transfection. (E-J) Differences in AAV vector genome quantity in cells during vector production. The raw values (E, G, and I) and fold differences (F, H, and J) in the AAV vector genome in cells during vector production of AAV2 (E, F), AAV5 (G, H), and AAV1 (I, J), respectively. All data were

independently performed at least three times and normalized with the value of the normal control (RC) samples. Asterisks in each panel indicate the following: * = $p < 0.05$, ** = $p < 0.01$. Error bars indicate the standard error of the mean.

Supplementary Figure 3. Full/empty particle ratio of the Tet-Cap system for various serotypes

(A-D) Western blot of capsid (Cap) protein after immunoprecipitation in various serotypes. The same titer of adeno-associated virus (AAV) vector (1×10^9-4×10^9 vg/sample) calculated using qPCR was subjected to immunoprecipitation using ADK1a (AAV1, AAV6), A20 (AAV3B), and ADK5a (AAV5) antibodies, as well as protein A and G magnetic beads, before western blotting. The left-hand figures show representative western blot images, and the right-hand figures the fold difference of band intensities for VP1, VP2 and VP3 proteins between the normal control (RC) and Tet-Cap samples in each panel. These panels indicate the data for AAV1 (A), AAV3B (B), AAV5 (C), and AAV6 (D), respectively. Experiments were independently performed at least three times for statistical analysis. Asterisks in each panel indicate the following: * = $p < 0.05$. Error bars indicate the standard error of the mean.

Supplementary Figure 4. Infectivity of AAV vectors produced using the novel vector production system

(A-D) Infectivity data of the AAV vectors for various serotypes *in vitro*. The 2v6.11 cells were infected with AAV1 (500 vg/cell), AAV3B (500 vg/cell), AAV5 (500 vg/cell), and AAV6 (500 vg/cell). Cells were observed 96 h post-infection. Data indicate infectivity of the AAV vector (EGFP; green) in AAV1 (A), AAV3B (B), AAV5 (C), and AAV6 (D). The blue signal shows nuclei (Hoechst 33342). White bar shows 100 μm. Data indicate representative images from three independent experiments.

Supplementary Figure 5. AAV vector production in large scale

(A) Adeno-associated virus (AAV) vector yield in T225 flasks using the Tet-Cap2 system. Fold differences in AAV vector yield for AAV2 between the normal control (RC2) and Tet-Cap systems after a change in medium and doxycycline stimulation 12 h post-transfection. (B) Western blot of capsid (Cap) proteins after immunoprecipitation in the T225 flask. The same titer of AAV vector calculated using qPCR was subjected to immunoprecipitation using A20 antibodies and protein A and G magnetic beads before western blotting. Cap and β-actin proteins were detected using anti-Cap and anti-β-actin antibodies, respectively. Figures show representative western blotting images. (C)

Infectivity data for AAV2 vectors produced in T225 flasks *in vitro*. The 2v6.11 cells were infected with AAV2 (1000 vg/cell) and observed 96 h post-infection. Data indicate infectivity of the AAV2 vector (EGFP; green) produced using the RC2 and Tet-Cap2 systems in T225 flasks. The blue signal shows nuclei (Hoechst 33342). White bar shows 100 μm. (D) Direct western blotting data of the AAV vector solutions. Control purified AAV2 vector purchased from Addgene and AAV2 vectors produced by normal and Tet-Cap systems were directly subjected to western blotting after lysis with 1× sodium dodecyl sulphate sample buffer. Figures show representative western blotting images. (E) Band intensity analysis data for the VP1:VP2:VP3 ratio obtained from the western blotting analysis in panel D. Data were normalized with the VP1 band intensity value. Circles, squares, and triangles show data of different batches of the control, RC2, and Tet-Cap samples. (F) AAV vector yield in 4-layer cell factory flasks for the Tet-Cap9 system. Fold differences in AAV vector yield for AAV9 between the normal control (RC9) and Tet-Cap9 systems after a change in medium and doxycycline stimulation 12 h post-transfection. Experiments were independently performed at least three times for statistical analysis. Error bars indicate standard error of the mean.

Supplementary Figure 6. Improvement of AAV vector genome replication by

changing the Rep78/Rep52 expression ratio

Differences in AAV vector genome quantity in cells during vector production using various replicase (Rep) constructs. Raw values (A) and fold differences (B) of the AAV vector genome in cells during AAV vector production. Data were normalized with measurements of the normal control (RC) samples. Experiments were independently performed at least three times for statistical analysis. Asterisks in each panel indicate the followng: * = $p < 0.05$. Error bars indicate standard error of the mean.

Supplementary Figure 7. Effect of Tet-stimulation timing on AAV vector production in stable HEK293 cells

(A) AAV vector yield (vg/μL) after doxycycline (Dox) stimulation timing in a clone (C4) of HEK293 cells carrying Tet-Cap2. (B) Fold differences in capsid (Cap) proteins measured using ELISA after stimulation of Cap expression at 12 and 24 h in C4. (C) Fold differences in qPCR/ELISA ratios corresponding with the full/empty particle ratio after stimulation of Cap expression at 12 and 24 h in C4. Data were normalized with the value of 0 h Dox stimulation sample. Experiments were independently performed at least three times for statistical analysis. Asterisks in each panel indicate the following: * = $p < 0.05$. Error bars indicate the standard error of the mean.

Supplementary Figure 1. Transfection efficiency between normal and Tet-Cap system during AAV vector production

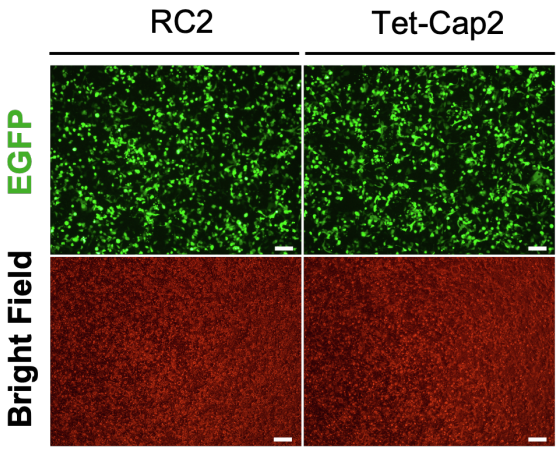

Supplementary Figure 2. Effect of AAV vector production in the Tet-Cap system for various serotypes

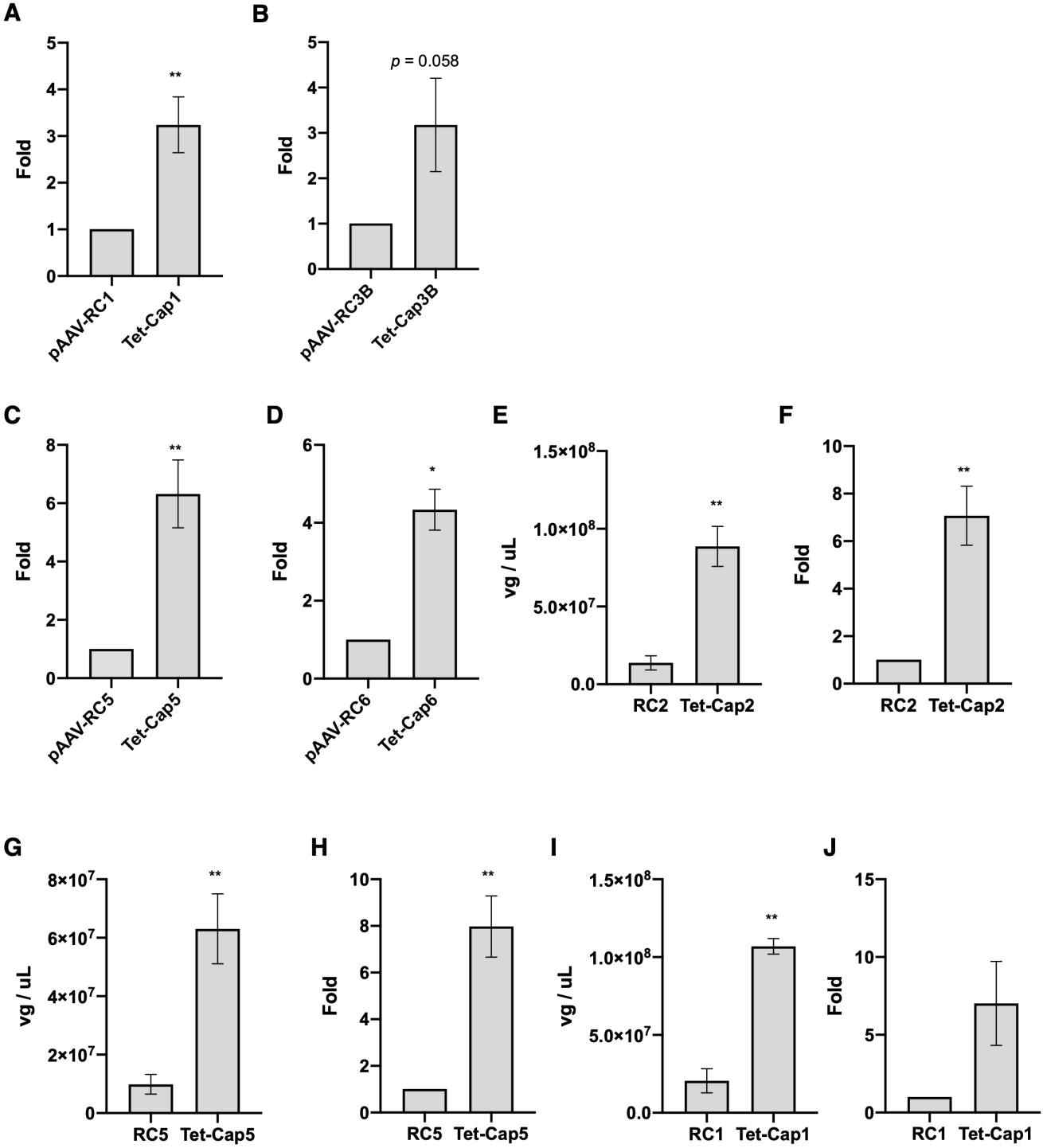

Supplementary Figure 3. Full/empty particle ratio of the Tet-Cap system for various serotypes

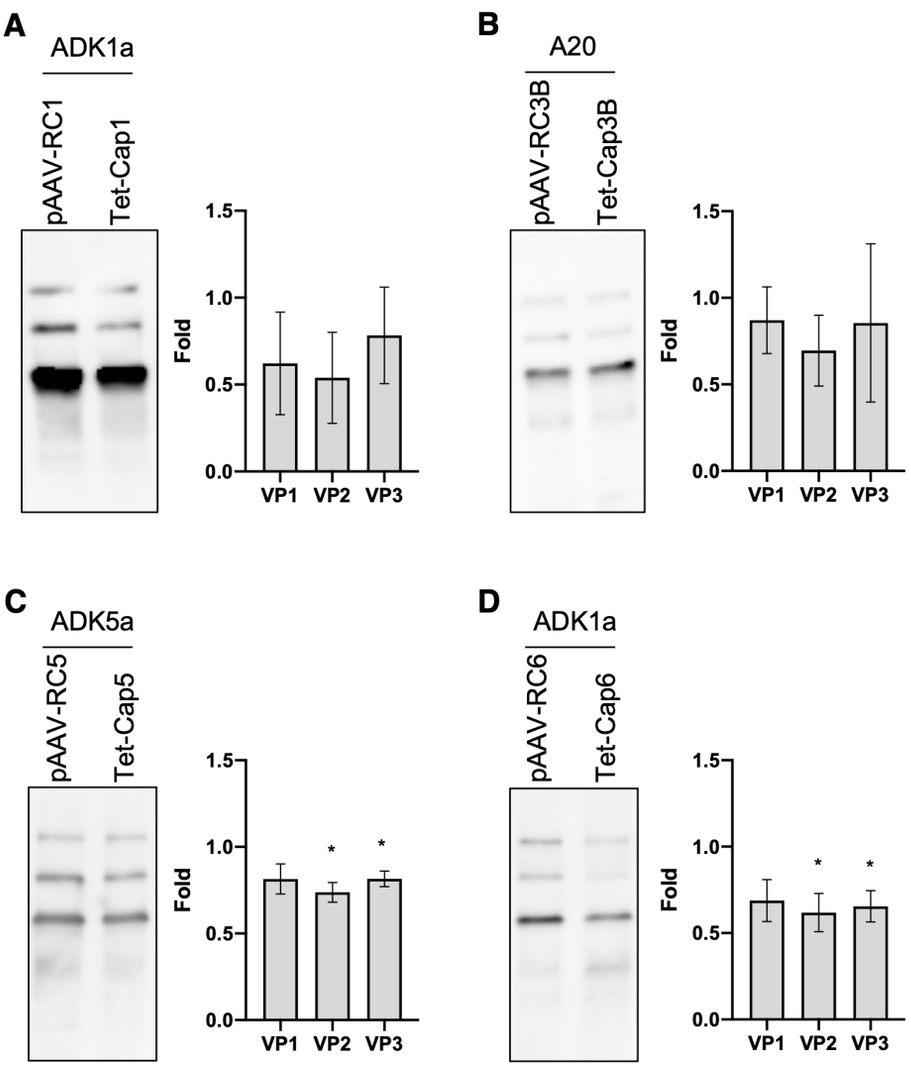

Supplementary Figure 4. Infectivity of AAV vectors produced using the novel vector production system

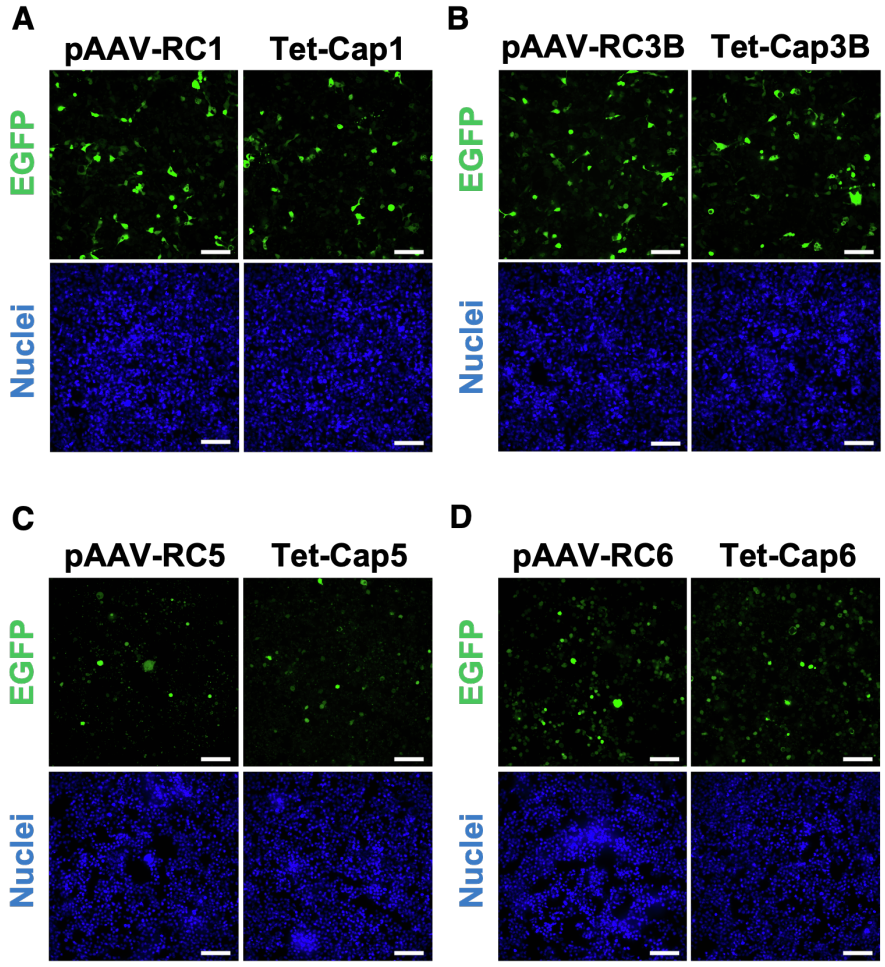

Supplementary Figure 5. AAV vector production in large scale

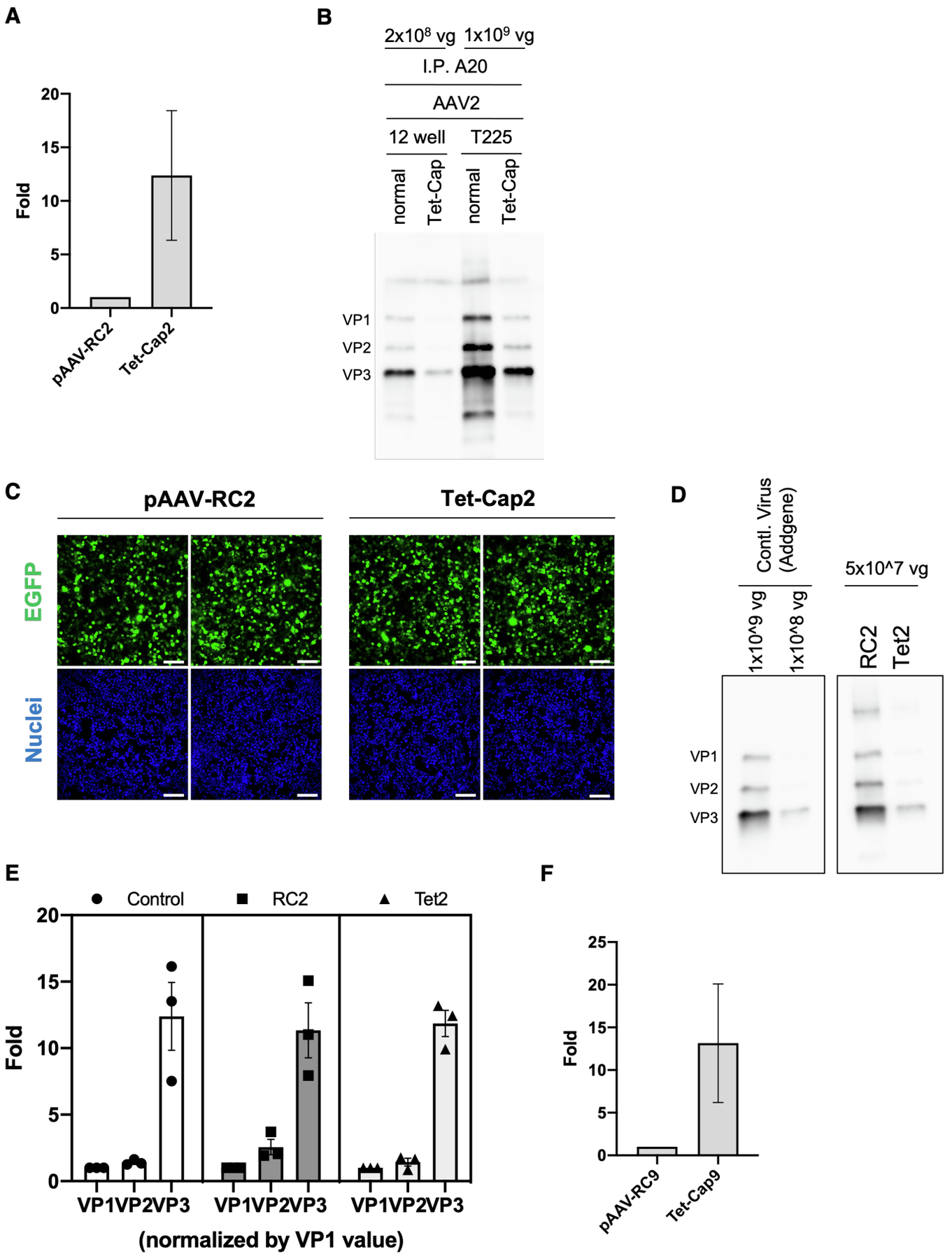

Supplementary Figure 6. Improvement of AAV vector genome replication by changing Rep78 / Rep52 expression ratio

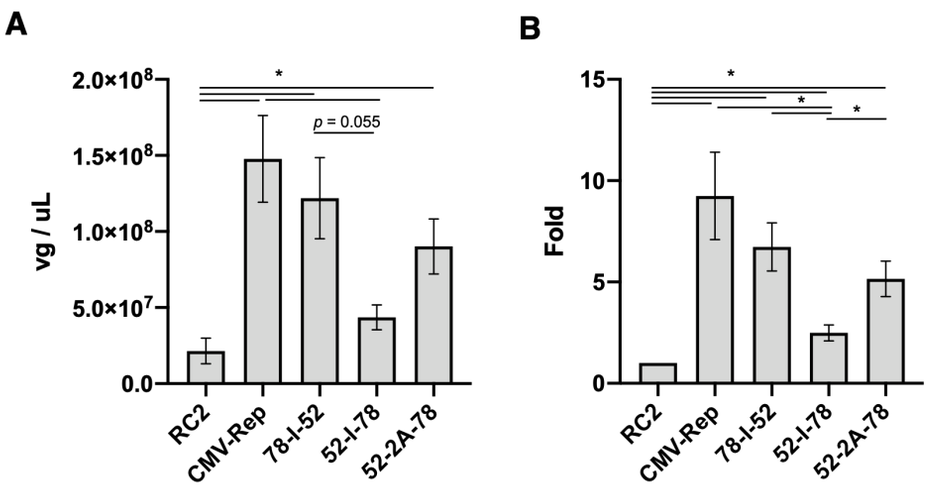

Supplementary Figure 7. Effect of Tet-stimulation timing on AAV vector production in stable HEK293 cells